I. STEADY-STATE KINETIC MECHANISM OF GLYCERALDEHYDE-3-PHOSPHATE DEHYDROGENASE

II. MAGNESIUM AND PROTON STABILITY CONSTANTS OF ORGANIC PHOSPHATE METABOLITES

By

EDWIN LUNG-FAT LI

Bachelor of Science

Oklahoma State University

Stillwater, Oklahoma

1975

Submitted to the Faculty of the Graduate College
of the Oklahoma State University
in partial fulfillment of the requirements
for the Degree of
Master of Science
December, 1977

I. STEADY-STATE KINETIC MECHANISM OF GLYCERALDEHYDE-3-PHOSPHATE DEHYDROGENASE

II. MAGNESIUM AND PROTON STABILITY CONSTANTS OF ORGANIC PHOSPHATE METABOLITES

Thesis Approved:

H. Olin Spivey
Thesis Adviser

Richard C. Essenberg

George V. Odell

Norman N. Durham
Dean of the Graduate College

ACKNOWLEDGMENTS

Gratitude is expressed to Dr. H. O. Spivey for his patience, advice, guidance and especially his tremendous help during the completion of the work for this thesis. In addition, gratitude is expressed to Drs. R. C. Essenberg and G. V. Odell, as advisory committee members, and to the biochemistry faculty. Appreciation is also extended to Drs. J. P. Chandler and D. D. Fisher of the Computer Science Department for computer analysis advice.

Appreciation is extended to Mr. Jim Appleman, who spent many long hours on the PRPP impurities determination.

Thanks is also extended to the Oklahoma State University Biochemistry and Chemistry Departments for financial support.

TABLE OF CONTENTS

LIST OF TABLES

LIST OF FIGURES

Figure Page

PART ONE

PART TWO

LIST OF SYMBOLS AND ABBREVIATIONS

χ = Greek Chi

Σ = Greek capital sigma, indicating summation

σ = Greek lower case sigma, indicating standard deviation

ν = Greek nu, indicating degrees of freedom

G3PD = Glyceraldehyde-3-phosphate Dehydrogenase

G3P = Glyceraldehyde-3-phosphate

DPG = Diphosphoglycerate

P_i = Inorganic phosphate

NAD^+ = β-Nicotinamide Adenine dinucleotide

NADH = β-Nicotinamide Adenine dinucleotide, reduced form

Q^+ = Quaternary ammonium ion

tpaBr = Tetrapropylammonium bromide

R5P = Ribose-5-phosphate

RDP = Ribose 1,5 diphosphate

ATP = Adenosine 5'-triphosphate

PRPP = 5-Phosphoribosyl-1-Pyrophosphate

PART ONE

STEADY-STATE KINETIC MECHANISM OF GLYCERALDEHYDE-3-PHOSPHATE DEHYDROGENASE

CHAPTER I

INTRODUCTION

Background and Objectives

D-Glyceraldehyde-3-Phosphate:NAD oxidoreductase (phosphorylating) (E.C.1.2.1.12) is a tetrameric glycolytic enzyme which catalyzes the reaction:

The steady-state kinetic mechanism of this enzyme (G3PD) is of particular interest because it has been investigated by several different research groups who came to different and apparently conflicting conclusions. Our interest in the mechanism of this enzyme stems from our previous study of the half-of-sites activity debate (1). Some of the conclusions of that study depend on the interpretation that NADH can rapidly dissociate from acylated enzyme. That is,

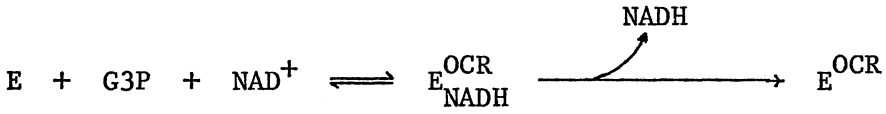

where E, and E^{OCR} are enzyme and enzyme thioester of 3-phosphoglycerate, respectively. The ordered steady-state mechanisms of Fahien (2) or Orsi and Cleland (3), however, only allow NADH to be released <u>after</u>

deacylation of the E^{OCR}_{NADH} complex, although Fahien's data do not exclude this possibility. They are the only ones of the proposals to be considered, which do not allow NADH release from the E^{OCR}_{NADH} complex.

Since these conclusions are contrary to those from other laboratories, Spivey suggested that the ordered pattern Orsi and Cleland observed might result from the high pH and/or pseudosubstrates which they used. To test this, Bartlett, Blanton, and Spivey (8) measured product inhibitions at pH 6.0, 7.0, and 8.6 with the natural substrates. As suspected, they found patterns characteristic of the ordered mechanism at pH 8.6, and of the random mechanism at pH 6.0, showing that pH alone could change the mechanism.

These results and other evidence on pH dependent rate constants (9, 10) suggest that some of the remarkably conflicting conclusions on the kinetic mechanism of this enzyme might be reconciled by considering the widely different pH values, substrates (natural- and pseudo-substrates), and sources of enzyme used. The objectives of this thesis, therefore, are to critically review the literature and to summarize what we consider to be the most important deficiencies in current data, and list our recommendations on studies to clarify the enzyme's mechanism. These include an analysis of steady-state kinetic theory to correct a misconception concerning product inhibition in rapid equilibrium ordered mechanisms.

Summary of Proposed Mechanisms

The major steady-state kinetic mechanisms proposed for this enzyme are summarized in Table I and Figure 1 in chronological order. Prior to these investigations, Segal and Boyer (4), studied the effects

TABLE I

PROPOSED MECHANISMS

Authors	Reference	Mechanism No. (Figure 1)	Conditions and Restrictions
Furfine and Velick (1965)	5	I	Rabbit muscle enzyme; pH 7.5; both reaction directions
Keleti and Batke (1965)	7	II	Pig muscle enzyme, pH 8.8; substrates G3P and glyceraldehyde
Fahien (1966)	2	III	Rabbit muscle enzyme, pH 8.0; glyceraldehyde (pseudosubstrate) oxidation only
Trentham (1971)	8,9	IV-A	Lobster and sturgeon enzyme, pH ~ 5→8; transient kinetic data only
Orsi and Cleland (1972)	3	V	Rabbit muscle enzyme; pH 8.6; pseudosubstrate oxidation only
Duggleby and Dennis (1974)	11	VI	Pea seed enzyme; pH 8.79; G3P oxidation only

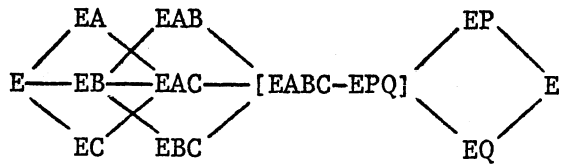

Furfine and Velick (I)

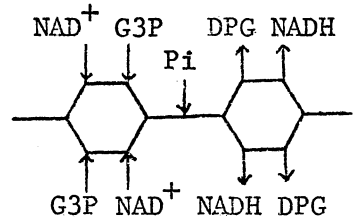

Keleti and Batke (II)[a]

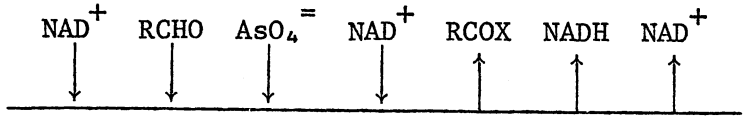

Fahien (III)

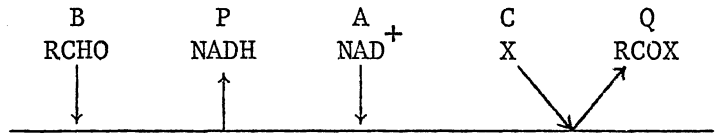

Trentham (IV-A[b])

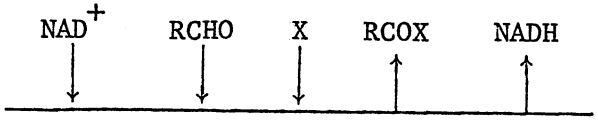

Orsi and Cleland (V)

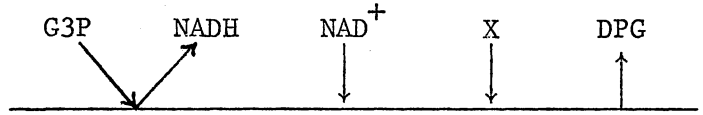

Duggleby and Dennis (VI)

[a]If glyceraldehyde is used instead of G3P, the mechanism becomes that of Furfine and Velick (I).

[b]Mechanism IV-B is the same as IV-A except that a two step deacylation replaces the Theorell-Chance X on RCOX off step.

Figure 1. Enzyme Mechanisms

of alkylating the enzyme's most reactive sulfhydryls, and the extents of reactions of substrate concentrations of enzyme (~ 5 μM) with G3P and NAD^+ without an acyl acceptor (R'OH) in reaction (4) (see below). They suggested the following reactions from their results:

$$RCHO + NAD^+\text{-E-SH} \rightleftharpoons NAD^+\text{-E-S-HOHCR} \quad (1)$$

$$NAD^+\text{-E-S-HOHCR} \rightleftharpoons NADH\text{-E-S-OCR} + H^+ \quad (2)$$

$$NADH\text{-E-S-OCR} + NAD^+ \rightleftharpoons NAD^+\text{-E-S-OCR} + NADH \quad (3)$$

$$NAD^+\text{-E-S-OCR} + X \rightleftharpoons NAD^+\text{-E-SH} + RCO\text{-}X \quad (4)$$

where X is an acyl acceptor (HPO_4^{2-}, $HAsO_4^{2-}$, or HOH). These reactions are not sufficient to specify a kinetic mechanism, however, since the release of both products, NADH and RCOX, are shown as biomolecular reactions (Theorell-Chance mechanism for product release), which would allow increasing reaction velocities with increasing substrate concentrations without limit.

Thus the first extensive kinetic study of the rabbit muscle enzyme was by Furfine and Velick (5) who concluded that the initial velocity kinetics at low enzyme concentration were best described by a random order of substrate addition to enzyme with the rate-limiting step occuring in the reaction of a kinetically important quaternary enzyme-substrate complex ([ ] in Mechanism I), namely, acyl group transfer from the enzyme to an external acceptor. Their mechanism (rapid equilibrium random ter-bi[1]) is summarized in Figure 1 where A,

---

[1]The terminology used for enzyme steady-state kinetics is that of Cleland (6).

B, and C are NAD^+, G3P, and phosphate; and P, Q, and E are NADH, DPG, and enzyme, respectively.

In agreement with this mechanism, the authors reported initial velocity patterns, which were all intersecting. Also all product inhibitions for both reaction directions were competitive, except for noncompetitive inhibition by NAD^+ with variable DPG.

Keleti and Batke (7) (Figure 1) came to very similar conclusions as Furfine and Velick. Fahien (2), however, proposed an ordered addition of substrates to catalytic sites in the sequence, NAD^+, RCHO, $HAsO_4^{2-}$, then a second NAD^+ to a "loose" binding site on a separate subunit (Mechanism III, Figure 1). Trentham (8, 9) has made extensive fast kinetic measurements on the reactions of lobster and sturgeon enzymes. These enzymes were chosen for their special physical and chemical properties, and the known structural features of the lobster enzyme. Based on these studies, which quantitate the enormous NAD^+ stimulation of both forward and reverse reactions, he proposed a ping-pong mechanism (IV-A in Figure 1).

Orsi and Cleland (3) next studied the rabbit muscle enzyme at pH 8.6, utilizing pseudosubstrates extensively. They concluded that the mechanism was ordered ter-bi reaction as shown in Figure 1 (Mechanism V).

The most recent study of the enzyme is that of Duggleby and Dennis (11), who used the enzyme from pea seeds at pH 8.79 exclusively. Their steady-state data and conclusions support the mechanism proposed by Trentham except they assume a Theorell-Chance release of NADH rather than DPG (Figure 1, Mechanism VI). A Theorell-Chance release of both

products is not possible since this would allow infinite velocity at infinite substrate concentrations, as mentioned above.

CHAPTER II

EVALUATION OF PROPOSED MECHANISMS

Are the Different Mechanisms the Result of Different Conditions?

Although the mechanisms proposed appear fundamentally conflicting, one could consider that many of them are expressions of only the dominant pathway under the conditions of pH, substrates (natural- or pseudo-), and source of enzyme used, which differ for nearly all studies. In this view, most substrates and products may add to or leave the enzyme surface randomly subject to the chemical reactions 1 through 4 above. For example, NAD^+ and G3P must, at some time, be on the enzyme simultaneously to permit oxidation of G3P, but the acyl acceptor substrate, X, may add before or after release of NADH, depending on pH and concentration of X. A dominant steady-state mechanism may then change to a considerable extent with conditions. An experimental test of this hypothesis requires that the dominant paths be established on a single enzyme at each condition of pH and choice of substrates. Although ample data support the view that a <u>given</u> kinetic pattern does change with pH (8-10), the data are far too limited to establish the full sequence of reactant additions and releases to and from the enzyme at each pH (the "steady-state kinetic mechanism"). We do not imply

that all features of the enzyme's mechanism may change with conditions. Specifically, it is unlikely that the covalent reactions will change fundamentally with pH or substrate. Thus, if the enzyme is known to involve reaction 2 above at pH 8.4, it is unlikely to use the mechanism,

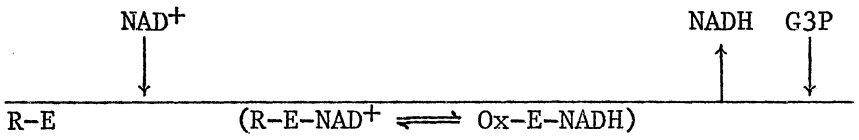

with redox reactions between the substrates and an enzyme group, R-, and Ox-, under any other conditions. Otherwise, numerous alternative paths may exist in principle.

There are some kinetic results with this enzyme, however, which appear constant in spite of different pH values or different substrates. Also certain measurements are less subject to artifacts than others. For example, since the reaction equilibrium is very unfavorable for G3P oxidation, initial velocities measured in this direction may be in large error unless DPG is kept at very low concentrations by coupling it to the 3-phosphoglycerate kinase reaction. Unfortunately only Duggleby and Dennis (11) use this precaution and neither they nor most others study the reverse direction. There remains some data, however, which is observed at both high and low pH and appears free of artifacts. We believe it is important to consider these results and the concept of alternative pathways, to see what kinetic mechanism is implied for this enzyme from present data. The features which we consider best established are the following:

1) Competitive product inhibition between NADH and G3P was found: with the rabbit enzyme at pH 7.4 for both reaction directions (5), and with the pea seed enzyme at pH 8.79 for G3P oxidation (11). No data exist on the pea seed enzyme for the reverse reaction. Orsi and Cleland (3), do describe noncompetitive inhibition by NADH with respect to the pseudosubstrate 3-hydroxy-propionaldehyde-3-P with the rabbit enzyme at pH 8.6, but the intercept effects are small and possibly artifacts.

2) Intersecting Lineweaver-Burke (L-B) plots of initial velocity data are observed with the enzyme from rabbit or pig (both reaction directions) (5, 7). Duggleby and Dennis (11) found parallel lines for G3P oxidation with the enzyme from pea seeds. Since, however, a sequential mechanism will appear to have parallel initial velocity L-B lines if $K_a >> K_{ia}$ (12), this observation of Duggleby and Dennis is not as definitive as are the observations of intersecting lines.

3) NAD^+ stimulates the enzymatic reaction in both directions (13, 8, 9). Trentham's measurements on sturgeon and lobster enzymes (8, 9) indicate that NAD^+ increases the rates of four of the elementary steps as much as 10^4 times. These steps are: phosphorolysis of acyl-enzyme; formation of acyl-enzyme from DPT + enzyme, and the formation and breakdown of enzyme-G3P complex. Only in the presence of NAD^+ do these reaction rates equal or exceed the enzyme turnover rate.

4) For G3P oxidation, the release of DPG (phosphorolysis) is rate limiting below a pH of about 8.0, while NADH release is rate limiting above a pH of 8.0 (9).

Remaining Deficiencies

It would appear necessary then to retain the feature of NAD^+ stimulation which the Fahien, Trentham, and Duggleby-Dennis mechanisms (III, IV, and VI, respectively) have. Fahien has only initial velocity data for glyceraldehyde oxidation, and Trentham has no steady-state data. Thus both studies, while giving valuable insights on the effects of NAD^+, do not distinguish the remaining possible mechanisms. To what extent, however, are these three mechanisms comparible with the other three observations which we are considering most reliable?

Of these three, only the Fahien mechanism allows intersecting initial velocity patterns, but neither the Fahien nor Trentham scheme appear to allow competitive product inhibition between NADH and G3P. The Duggleby-Dennis scheme does permit this competitive inhibition since the G3P-NADH sequence is assumed to be a Theorell-Chance mechanism (Ref. 12, p. 21), which is equivalent to assuming that the concentration of the intervening central complex is negligible. Since the data of Duggleby and Dennis are at pH 8.79, however, this assumption conflicts with data of Trentham indicating that NADH release is rate limiting at pH 8.0 and above (observation 4 above).

In summary, the inhibitions between NADH and G3P are mathematically noncompetitive in each of the three mechanisms, III, IV, and VI, which allow for the NAD^+ requirement for DPG reduction. Recognizing this, Trentham argues that if the steps of NAD^+ addition and phosphorolysis (the NAD^+, X, RCOX sequence in mechanism IV) are rapid relative to the slow addition of G3P (RCHO) in the mechanism, inhibition by NADH

will appear experimentally competitive. Duggleby and Dennis accept this view but we were skeptical. Since this is a critical argument in deducing mechanisms from steady-state kinetic data, our first objective was to demonstrate whether a rapid equilibrium condition, or any other special relation among the rate constants of mechanism IV, could make inhibition by NADH(P) appear competitive with G3P (B) in practice, though it is mathematically noncompetitive.

Product Inhibitions in Rapid Equilibrium Ordered Mechanisms

Methods

It was necessary to establish the effects of various rate constant values on the apparent steady-state patterns of Lineweaver-Burke (L-B) lines. Trentham argues that adjusting the rate constants for mechanism IV-A so that the reaction, $E^{OCR} + NAD^+ \rightleftharpoons E^{OCR}_{NAD^+}$ and $E^{OCR}_{NAD^+} + X \rightleftharpoons E_{NAD^+} + RCOX$ are in rapid equilibrium with the next reaction ($E_{NAD^+} + RCHO \rightleftharpoons E^{RCHO}_{NAD^+}$), will make inhibition by P appear competitive with B. In this case, the P terms in the intercepts of L-B equations will be negligible relative to the other terms in the intercept while P terms in the slopes will remain significant.

Trentham's hypothesis was tested by a combination of theoretical derivations and computer simulations. Exact steady-state equations were derived by the computer program of Fisher and Schulz (14) for mechanisms to be examined. IBM CPS computer programs were then written to calculate slope and intercept terms of Lineweaver-Burke plots for various specified input conditions of substrate and product

concentrations, and rate constants. This permits rapid simulation on our time sharing computer terminal of the enzyme kinetic behavior for any mechanism. Rate constants were varied within the limits set by the following constraints: bimolecular rate constants < 10^9 M^{-1} s^{-1}, the diffusion limited rate constant (15); unimolecular rate constants $\geq$ catalytic center activity (enzyme turnover number in s^{-1}). Further details of the program are given in Appendix A.

Results and Conclusions

A sufficient condition to make the $E + A \underset{k_2}{\overset{k_1}{\rightleftharpoons}} EA$ reaction in equilibrium with the next reaction, $EA + B \underset{k_4}{\overset{k_3}{\rightleftharpoons}} EAB$, in the steady-state kinetics of a two substrate ordered enzyme mechanism is $k_2 >> V_m/(E_t)(V_m/(E_t) \equiv$ the rate limiting rate constant) (13). That is the reverse rate constant of the equilibrium reaction must be large relative to the rate limiting rate constant. Since at equilibrium of the first reaction, $(E) = \frac{k_2}{k_1(A)}(EA)$, and infinite (B) decreases (EA) to zero, (E) will also be decreased to zero by infinite (B). It follows then that inhibition by any inhibitor acting on E will be eliminated by $(B) \rightarrow \infty$. Thus such inhibitions will <u>appear</u> competitive with B in practice, although they are mathematically noncompetitive with B.

Trentham extended this idea to his proposed mechanism IV-A or B to explain the competitive inhibition between P and B. It did not seem possible to us, however, that the reactions between additions of P and B in Trentham's mechanism IV-A or B, e.g., the A C Q sequence in mechanism IV-B, could satisfy the criteria for equilibria

of sequential reactions, since these reactions include release of product, RCOX (Q), at zero concentration. To clarify this question, the reverse reaction constants for additions of A and C were increased to values much larger than V_m/E_t, and the L-B plots of the resulting equation computed. Changing the reverse reaction constant for release of Q (k_5' in Appendix B) could not affect the calculated intercepts, since k_5' does not appear in the intercept equation when RCOX (Q) is absent. As shown in Table II, however, increasing the rate constants for dissociation of A and C from their enzyme forms increased the effect of P on the intercepts, rather than reducing it as needed to make P inhibition appear competitive with B. Similar observations were obtained with mechanism IV-A. To clarify what condition on rate constants would reduce inhibitor effects on L-B intercepts, the steady-state equations for the bi-bi ordered and ping-pong mechanisms VII and VIII

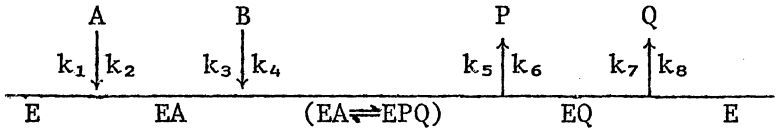

(VII)

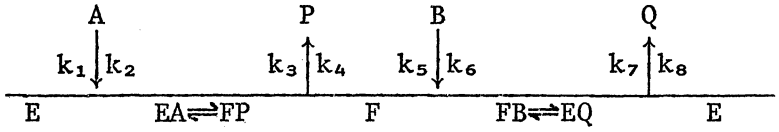

(VIII)

were analyzed. In order that inhibitions by P be competitive with B or A, however, the conditions making P terms negligible in the intercepts must not also make P terms negligible in the slopes, otherwise no inhibition by P will exist. Thus we examine intercepts and slopes for mechanisms VII and VIII.

TABLE II

EFFECT OF CHANGING REVERSE RATE CONSTANTS IN TRENTHAM'S MECHANISM IV-B ON THE INHIBITION BY NADH (= P)

Intercepts tabulated are for Lineweaver-Burke plots with variable RCHO (B). See Appendix II for reaction scheme, equations and definition of constants.

$k_2^1 = k_2^3 = k_4^3 = k_5^4 = 10^8\ M^{-1}\ s^{-1}$; $k_1^5 = 10^4\ s^{-1}$;

$k_1^2 = 80\ s^{-1}$; $k_5^1 = 2 \times 10^5\ M^{-1}\ s^{-1}$; $k_3^2 = 200\ s^{-1}$.

10^3 x Intercepts with $k_3^4 = k_4^5 = 100\ s^{-1}$				10^3 x Intercepts with $k_3^4 = k_4^5 = 10^4\ s^{-1}$			
P	NAD, μM			P	NAD, μM		
μM	10	50	100	μM	10	50	100
0	6.84	5.99	5.88	0	20.8	9.30	7.87
1	7.37	6.09	5.93	1	27.9	10.7	8.58
5	9.51	6.52	6.15	5	56.6	16.5	11.4

For mechanism VII, we have

$$\text{intercept} = \frac{1}{V_1}\left(1 + \frac{K_a}{A} + \frac{P}{K_{ip}}\right) \tag{1}$$

$$\text{slope} = \frac{K_b}{V_1}\left(1 + \frac{K_{ia}}{A}\right)\left(1 + \frac{K_q P}{K_{iq} K_p}\right) \tag{2}$$

In order to abolish the P term for all A in equation 1, $\frac{P}{K_{ip}} \ll 1$, and thus $K_{ip} \gg P$ must be satisfied. But $K_{ip} = \frac{k_1 k_3 (k_5 + k_7)}{k_1 k_3 k_6} = \frac{k_5 + k_7}{k_6}$, therefore, $k_5 + k_7$ must be much larger than $k_6 P$. Similarly for the slope (equation 2), the condition

$$\frac{K_q P}{K_{iq} K_p} = \frac{k_2 k_4 k_6 P / [(k_2 + k_4) k_6 k_8]}{k_7 k_2 (k_4 + k_5) k_8 / [k_8 (k_2 + k_4) k_6 k_8]}$$

$$= \frac{k_6 P}{k_7 \left(1 + \frac{k_5}{k_4}\right)} \ll 1$$

must be satisfied to remove effect of P. Thus we can see that the same condition (increasing k_5 and k_7 relative to $k_6 P$), which reduces intercepts will reduce slopes also. The percentage change in intercept for a given change in rate constants is nearly the same for slope. Thus it is unlikely that inhibition by P will appear competitive with B if P is at inhibiting levels at all.

For the ping-pong mechanism VIII, the necessary conditions for reducing the P terms are:

$$\text{Intercept P term} = \frac{k_4 k_6}{k_3 (k_5 + k_7)} \ll 1$$

$$\text{Slope P term} = \frac{k_2}{k_1} \times \text{Intercept P term} \ll 1$$

Again the same condition that abolishes the P term in intercept will abolish the P term in slope, and no inhibition will occur. It is true that the rates of change of intercepts and slopes with P, though similar, are not identical. Thus it is possible that the effects of P on intercepts might be negligible while they remain significant on slopes. From a preliminary consideration of this, we judge this possibility highly unlikely since it would require an unusual relation among rate constants and a narrow range of (P).

Trentham's mechanism (IV-A and B) for glyceraldehyde-3-P dehydrogenase is only slightly different from mechanism VIII, and the principles clarified above appear to exclude a competitive inhibition between P and B in Trentham's mechanism also. Nevertheless, the slopes and intercepts of the L-B equation were calculated for mechanism IV-B assuming first normal constants with which inhibition between P and B was noncompetitive, then with increased forward constants for the $\underline{\overset{A}{\downarrow}\quad\overset{C}{\downarrow}\quad\overset{Q}{\uparrow}}$ sequence. As shown in Table III, effects of P vanished from both slopes and intercepts in the latter case.

The above analysis demonstrated that a "rapid equilibrium ordered" sequence of substrates, $\underset{E}{\overset{A}{\downarrow}\quad\overset{B}{\downarrow}}$, will make inhibition by any inhibitor acting on <u>E</u> appear competitive with B. Yet the analysis suggest that inhibitors acting on any <u>enzyme•product</u> complex will remain noncompetitive in spite of this condition. It is profitable to explain the reason for this difference. The equilibrium of the $E + A \rightleftharpoons EA$ reaction by itself does not eliminate concentrations of enzyme•product, e.g., EQ with which P combines as

TABLE III

EFFECT OF CHANGING FORWARD CONSTANTS IN TRENTHAM'S MECHANISM IV-B ON THE INHIBITION BY NADH (= P)

$k_2^1 = 10^8\ M^{-1}\ s^{-1}$; $k_1^2 = 160\ s^{-1}$; $k_3^2 = 150\ s^{-1}$; $k_3^4 = 80\ s^{-1}$; $k_4^5 = 200\ s^{-1}$

PμM	NAD μM	Non-Rapid Equilibrium[a]		Rapid Equilibrium[b]	
		intercepts	10^8 x slope	intercepts	10^8 x slope
0	10	11.8	2.07	8.50	2.07
1	10	19.5	1.25	8.51	2.07
5	10	50.7	622.	8.54	2.07
0	50	2.48	2.07	7.66	2.07
1	50	4.03	251.	7.66	2.07
5	50	10.2	125.	7.66	2.07
0	100	1.31	2.07	7.55	2.07
1	100	2.09	12.7	7.55	2.07
5	100	5.20	62.4	7.56	2.07

[a] $k_2^3 = 10^8\ M^{-1}s^{-1}$; $k_4^3 = 10^5\ M^{-1}s^{-1}$; $k_5^4 = 10^6\ M^{-1}s^{-1}$; $k_1^5 = 200\ s^{-1}$; $k_5^1 = 10^8\ M^{-1}s^{-1}$.

[b] $k_2^3 = 10^6\ M^{-1}s^{-1}$; $k_4^3 = 10^8\ M^{-1}s^{-1}$; $k_5^4 = 10^8\ M^{-1}s^{-1}$; $k_1^5 = 10^4\ s^{-1}$; $k_5^1 = 10^5\ M^{-1}s^{-1}$.

a product inhibitor, since subsequent release of product (e.g., $EQ \rightarrow E + Q$) is necessarily rate limited by its unimolecular nature, in contrast to $E + A \rightarrow EA$. Thus substantial enzyme species other than free E remains with infinite (B). Presumably a sequence of equilibrium steps of substrate additions could exist in 3 or more substrate enzymes, which would make mathematically noncompetitive inhibitions of enzyme•substrate forms appear competitive with a subsequently added substrate, but noncompetitive inhibitions acting on enzyme•product forms will remain noncompetitive. If the rate constants of a mechanism are changed to make product release steps in equilibrium with some subsequent substrate addition step, however, this forces the very enzyme•product form inhibited by the product (or other inhibitor) to zero concentration, eliminating all inhibition.

Another way to demonstrate the difference between inhibitors acting on E and those acting on enzyme-product forms is to compare the intercept of L-B equation of the ordered bi-bi mechanism for P inhibition (acting on EQ) with variable B,

$$\text{Intercept}_P = \frac{1}{V_1}\left(1 + \frac{K_a}{A} + \frac{P}{K_{ip}}\right)$$

with the intercept for Q inhibition (acting on E) with variable B,

$$\text{Intercept}_Q = \frac{1}{V_1}\left[1 + \frac{K_a}{A}\left(1 + \frac{Q}{K_{iq}}\right)\right]$$

Imposing the condition for the rapid equilibrium ordered mechanism, $K_a = 0$, abolishes the inhibition term in Intercept_Q, but not in Intercept_P. The inhibition terms in the slopes are not affected in

either case, however.

We conclude that Trentham's, and Duggleby and Dennis's mechanism (VI) are incompatible with the data of Furfine and Velick (5) with rabbit muscle enzyme, as well as Duggleby and Dennis's data on the pea seed enzyme, which indicate competitive inhibition by P (NADH) with respect to B (G3P). We should also add that mechanism VI is incompatible with results of Bartlett et al. (10) showing competitive inhibition by diphosphoglycerate with respect to NAD^+.

Possible Explanations for Conflicting Conclusions from Published Studies

The latest study of the enzyme's mechanism is by Duggleby and Dennis who review the earlier work, and offer excellent criticisms of some of the earlier experimental methods and data. All of their data are consistent with their proposed mechanisms. Two results from earlier workers, which they are unable to criticize, however, conflict with their mechanism, and they have not done the comparable experiments. First, the intersecting initial velocity data with NADH and DPG of Furfine and Velick conflict with their mechanism. Second, although they avoid conflict with their own data and those of others (competitive inhibition by NADH with respect to G3P) by invoking a rapid release of NADH (the Theorell-Chance step of G3P on, NADH off), this conflicts with Trentham's data (5), which indicates that NADH release is the rate limiting step above a pH of 7.8.

None of the mechanisms proposed, therefore, are compatible with what appears to be valid data from the other studies considered. A partial reduction in conflicts is accomplished by considering that

alternative steady-state paths exist in the mechanism of a single enzyme (same biological origin). Random path mechanisms do exist for several enzymes, and contrary to popular views, the fraction of flux which passes through each path can be altered by both pH and changes in substrates. A random pathway at one pH can appear ordered at another pH as demonstrated for glyceraldehyde-3-phosphate dehydrogenase (10). Steady-state mechanisms on enzymes are rarely established except at one pH. We believe, therefore, that there has been unwarranted faith in the invariance of a steady-state mechanism of a given enzyme under different solution conditions, or with different (pseudo-) substrates. In fact we would guess that changes in the order of substrates added and products released at different pH values would be especially prevalent for organic phosphate substrates, as with glyceraldehyde-3-phosphate dehydrogenase, if there is even slight flux through an alternate, but minor pathway at one pH.

These ideas are illustrated in Figure 2, which includes most of the pathways proposed (see Table I also). At pH of 8.0 and above, phosphate exists nearly completely as the dianion, which is the natural substrate form (8). Thus NADH (P) release rather than phosphorolysis is the rate limiting step (8) and thus most of FP in Figure 2 is likely to go to FPC $\longrightarrow$ EP (Cleland's path) rather than through the alternate path FP $\longrightarrow$ F + P. The opposite is true at lower pH values. Changes in rates of addition and release of G3P and DPG would also be expected. Since so many paths and phosphate reactants exist, the prediction of which paths may assume a dominant role as pH is changed is very difficult.

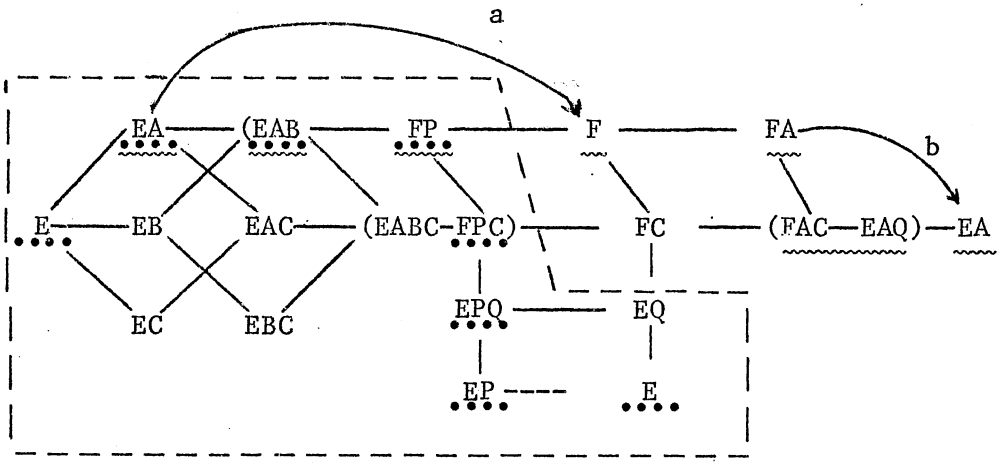

•••• Cleland

~~~~ Trentham, Duggleby and Dennis

Furfine and Velick

A = NAD^+; B = G3P; C = HPO_4^{2-}

P = NADH; Q = DPG

F = E^{SOCR}

[a]Possible only at low pH, Theorell-Chance step by Duggleby and Dennis.

[b]Possible only at high pH, Theorell-Chance step by Trentham.

Figure 2. Alternate Pathways for the Reactions of Glyceraldehyde-3-Phosphate Dehydrogenase
~~~~

Initially we thought it possible to rationalize the major mechanisms in terms of a consistent pattern of shifting pathways with the various pH and substrates used. This seems unlikely now, and even premature. It seems wiser to point out deficiencies in existing data in hopes that this will prompt further experiments. In addition to changes in pH and substrates, most investigators prefer to use their own source of enzyme; four different ones in the six major studies in Table I! Trentham carefully considers the different kinetic and physical properties of enzymes from several sources including yeast, sturgeon, lobster, and rabbit muscle before choosing the sturgeon and lobster enzymes for further study (9). Yet in the latest study, Duggleby and Dennis simply state, "This enzyme (from pea seeds) appears to be essentially identical to glyceraldehyde-3-phosphate from other sources.", with no reasons given for this apparently a priori faith in results not yet established.

CHAPTER III

SUMMARY AND RECOMMENDATIONS

We suggest the following are the most profitable approaches to clarify the glyceraldehyde-3-phosphate dehydrogenase mechanism.

1) Gather all data on the same enzyme at the same pH, and with natural- not pseudo- substrates. The reasons Trentham gives for choosing sturgeon and lobster enzymes is persuasive (9).

2) A pH nearer cytoplasm values is preferable to higher values for two reasons. First, G3P is more stable (11), and second, the results are more immediately physiologically pertinent. The difficulty avoided at pH 8.79 by Duggleby and Dennis (11) of the smaller linear extent of initial velocity at pH 7.4, should be more than compensated for by using a sensitive fluorescence detector, and full time progress curve analysis as Frieden has done with malate dehydrogenase for similar reasons (16). Alternatively, or in addition, 3-phosphoglyceric acid kinase and ADP can be used to keep the reverse reaction from interfering.

3) Initial velocity and product inhibition data with DPG should be obtained. We do not believe the instability of this substrate is large enough to cause noticeable errors within several hours (perhaps a day) to prevent these critically needed data. Its preparation is relatively easy (17).

4) Kinetic data should be obtained at enzyme concentrations

where the extent of enzyme association is constant; preferably at its native state, if feasible. Gel filtration techniques can establish the oligomeric state of the enzyme even at concentrations less than 1 μg enzyme/ml. Laser light scattering techniques are quicker and suitable for small volumes of more concentrated protein. Progress curve analyses should reduce quantities of enzyme needed relative to initial velocity reaction data.

5) Isotope exchange kinetics at reaction equilibrium would probably establish the presence or absence of alternative paths most sensitively.

6) In the past, conflicting data of previous workers was often not experimentally considered if it could not be rationalized. It seems wiser to at least do the comparable experiment. In any event, evidence concerning prefered intermediates of another enzyme or at another pH should not be assumed valid for the enzyme under study, or valid at different pH values.

The above experiments assume that the kinetics of this enzyme obey Michaelis-Menten equations (linear Lineweaver-Burke plots). Specifically the assumptions are made that: 1) for studies with substrate concentrations >> enzyme concentration, there are no interactions between subunits which would cause nonlinear kinetics, and 2) there are no steady-state random paths which will give erroneous L-B plots, as described for phosphofructokinase (18). The first assumption is often justified by the argument that over the range of substrate concentrations used, all subunits but the fourth remain saturated with substrates and hence no changes occur in the kinetic constants as the substrate concentrations are varied. When

enzyme and substrate concentrations were both very low, however, the observed kinetics were very nonlinear (19). This was thought to be (19) the result of varying extents of saturation of several enzyme subunits, which because of the highly cooperative subunit interactions caused nonlinear kinetics. The second assumption is also accepted without question because "linear kinetics" are observed. Actually, however, linear kinetics on this enzyme are only observed over a quite small range of substrate concentrations, and any continuous function will appear linear over a sufficiently small range of the independent variable. Thus the validity of both of the above assumptions are questionable. It would be wise to seek direct evidence for these assumptions, and keep these reservations in mind. Isotope exchange kinetics might validate assumption 2. Further stopped-flow studies at enzyme concentrations where enzyme-substrate complexes may be monitored spectrophotometrically might clarify questions on assumption 1, though this assumption would appear more difficult to verify.

Presently, however, we do not have a single mechanism explaining the kinetic properties of any one of these enzymes. Even the steady-state kinetics studies as suggested in items 1) through 6) above, however, should be valuable in clarifying many questions, and possibly achieving a valid mechanism. If the steady-state mechanism of this enzyme could be clarified, we believe it would enhance our understanding of its physiological properties substantially, and enlighten us concerning molecular mechanisms of enzyme catalysis. Perhaps as significantly, this accomplishment should teach us many

lessons on how and how not to pursue further studies with similar objectives on other enzymes.

A SELECTED BIBLIOGRAPHY

(1) Peczon, B. D., and Spivey, H. O. (1972) Biochemistry 11, 2209-2217.

(2) Fahien, L. A. (1966) J. Biol. Chem. 241, 4115-4123.

(3) Orsi, B. A., and Cleland, W. W. (1972) Biochemistry 11, 102-109.

(4) Segal, H. L., and Boyer, P. D. (1953) J. Biol. Chem. 204, 265-281.

(5) Furfine, C. S., and Velick, S. F. (1965) J. Biol. Chem. 240, 844-855.

(6) Cleland, W. W. (1963) Biochim. Biophys. Acta 67, 173-187.

(7) Keleti, T., and Batke, J. (1965) Acta Physiol. Hung. 48, 195-207.

(8) Bartlett, R. T. (1974) M.S. Thesis, Department of Biochemistry, Oklahoma State University, Stillwater, Okla.

(9) Trentham, D. R. (1971) Biochem. J. 122, 59-69.

(10) Trentham, D. R. (1971) Biochem. J. 122, 71-77.

(11) Duggleby, R. G. and Dennis, D. L. (1974) J. Biol. Chem. 249, 167-174.

(12) Cleland, W. W. (1970) in The Enzymes (Boyer, P. D., ed.) Vol. II, pp. 1-65, Academic Press, New York.

(13) De Vijlder, J. J. M., Hilvers, A. G., Van Lis, J. M. J., and Slater, E. C. (1969) Biochim. Biophys. Acta 191, 221.

(14) Fisher, D. D., and Schulz, A. R. (1969) Mathematical Biosciences 4, 189-200.

(15) Eigen, M., and Hammes, G. G. (1963) Adv. Enzymol. 25, 1-38.

(16) Frieden, C., and Fernandez-Souza, J. (1975) J. Biol. Chem. 250, 2106-2113.

(17) Negelein, E. (1957) in Methods of Enzymology (Colowick, S. & Kaplan, N., eds.), Vol 3, p. 216, Academic Press, New York.

(18) Bar-Tana, J., and Cleland, W. W. (1974) J. Biol. Chem. 249, 1263-1270.

(19) Smith, C. M., and Velick, S. F. (1972) J. Biol. Chem. 247, 273-284.

APPENDIXES

APPENDIX A

CPS PROGRAM TO CALCULATE SLOPE AND INTERCEPT TERMS OF LINEWEAVER-BURKE PLOTS

The intercept (and slope) terms of Lineweaver-Burke (L-B) plots were calculated on the IBM time sharing CPS terminal as follows:

1. A set of rate constants consistent with the constraints given in Chapter II under Methods were specified, and a HPO_4^{2-} = C concentration was chosen.

2. A range of NADH = P concentrations was chosen.

3. A range of NAD^+ = A concentrations was chosen.

4. Each of the intercept (and slope) terms were then calculated for each NAD^+ concentration with a given NADH concentration.

5. NADH concentrations were incremented and step 4 repeated until all NADH concentrations were used.

6. Changes in any of the rate constants desired were made and all steps of 3 and 4 repeated. This was continued until the effects of the rate constants on the intercepts (and slopes) was clear.

APPENDIX B

EVALUATION OF SLOPE AND INTERCEPT TERMS

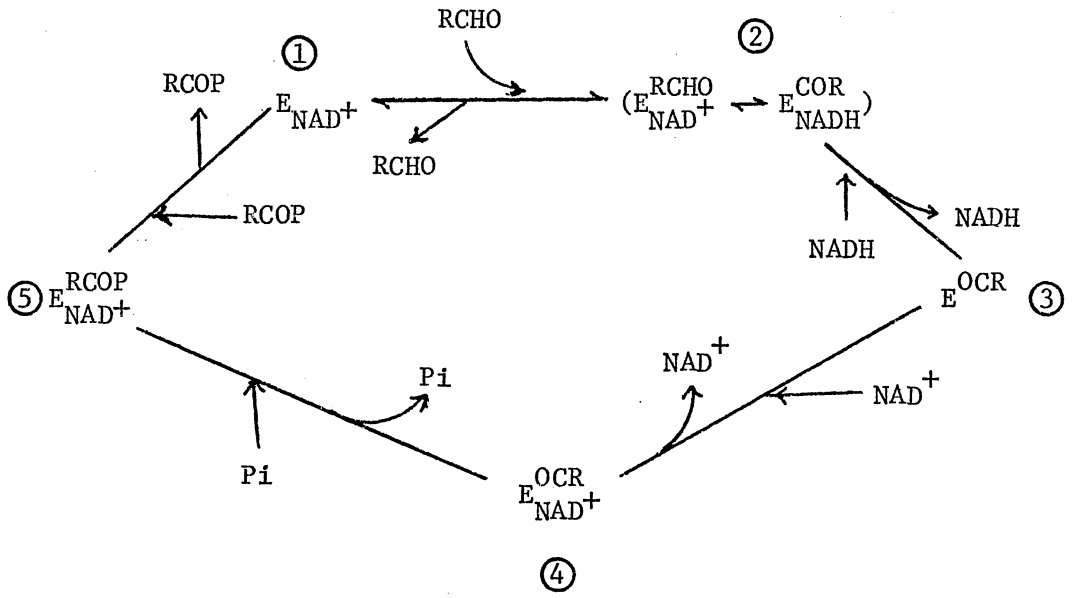

$$INT^a = \left(\sum_{i=1}^{6} Term_i\right)/NUM; \quad SLOPE = \left(\sum_{i=7}^{9} Term_i\right)/NUM;$$

$$Term_1 = \frac{(Coef_B)}{AC}; \quad Coef_B = k_2^1k_3^2k_3^4k_4^5 + k_2^1k_3^2k_3^4k_1^5$$

$$Term_2 = \frac{(Coef_{BP})^P}{AC}; \quad Coef_{BP} = k_2^1k_2^3k_3^4k_1^5 + k_2^1k_2^3k_3^4k_4^5$$

$$Term_3 = \frac{(Coef_{BC})}{A}; \quad Coef_{BC} = k_2^1k_3^2k_5^4k_1^5$$

$$Term_4 = \frac{(Coef_{BCP})^P}{B}; \quad Coef_{BCP} = k_2^1k_2^3k_5^4k_1^5$$

$$Term_5 = \frac{(Coef_{AB})}{C} \; ; \quad Coef_{AB} = k_2^1k_3^2k_4^3k_4^5 + k_2^1k_3^2k_4^3k_1^5$$

$$Term_6 = (Coef_{ABC}); \; Coef_{ABC} = k_2^1k_3^2k_5^4k_1^5 + k_2^1k_1^2k_4^3k_5^4$$

$$Term_7 = (Coef_{AC})$$

$$Term_8 = (Coef_P)P/AC$$

$$Term_9 = (Coef_{PC})P/A$$

$$NUM = k_2^1k_3^2k_4^3k_5^4k_1^5$$

where A = NAD^+, B = G3P, C = X(HOP_4^{2-} or $HAsO_4^-$), and P = NADH

$^a_{INT}$ - intercept

PART TWO

Mg^{2+} AND H^{+} STABILITY CONSTANTS OF ORGANIC PHOSPHATE METABOLITES

CHAPTER I

INTRODUCTION

5-Phosphoribosyl-1-pyrophosphate (PRPP) is a biologically active compound which is involved in the direct formation of purine and pyrimidine nucleotides from free bases. It is also significant in the biosynthetic pathways of tryptophan, histidine, and nicotinamide coenzymes. Since free Mg^{2+} concentrations in the cell are about 1 mM (1), PRPP would be expected to exist extensively as a Mg-PRPP complex *in vivo*. In analogy to ATP and ADP, we would also expect that the Mg-PRPP complex would be the true enzyme substrate in most of its enzymatic reactions. Experimental results support this view (2-5). In order to plan proper enzyme kinetic studies on metal-ligand substrates it is necessary to know the metal-ligand stability constants. At pH values below 8.0, the proton competes with the divalent metal ion for the ligand, hence it is also necessary to know the proton-ligand stability constants for experiments below pH 8.0. Neither of these constants are known for PRPP. This surprising fact is probably due to the past cost, poor quality, and instability of commercial preparations. Improvements in the commercial preparation, however, and our interest in enzymes utilizing PRPP motivated us to measure its Mg^{2+} and H^{+} stability constants. We have used the pH titration method (6, 7) since it

provides both metal and proton stability constants, which permit calculation of equilibria valid at all pH.

The measurements have been made on three different PRPP preparations. The first determinations were made by Thompson (6). He used commercial PRPP, which was further purified by the method of Khorana et al. (8) to give the Li_5-PRPP salt. To obtain accurate stability constants in a physiological medium of potassium and sodium chloride, it was necessary to correct for the lithium-phosphate complexes, which have higher stability constants than the Na^+ and K^+ complexes. After completing these measurements, we learned that Mohan and Rechnitz (9, 10) had raised serious doubts about the accuracy of literature values of metal ion stability constants. They claimed that previous estimates of the stability constants for alkali metal ion complexes at 0.2 M ionic strength were as much as 7 times too low. This uncertainty would make corrections to our PRPP data highly questionable.

Thus a second determination was made by Ms. L. S. Blanton on sodium PRPP as obtained commercially without further purification. Subsequently Ms. K. S. McGurk and Mr. James R. Appleman developed a reliable method of determining the identity and quantity of impurities in PRPP samples (see under Experimental). Since there was doubt about the effects of impurities in Ms. Blanton's experiments, we have used a PRPP sample, whose impurities were measured, for a third determination of stability constants.

Mohan and Rechnitz (9) contend that the errors in previous measurements are the result of inaccuracies in the pH titration method, or due to binding of the quartenary ammonium ions (used to

adjust ionic strength to 0.200 M) to the organic phosphates, or both reasons. Since we use the pH titration method, which has several advantages, and the quaternary ammonium ions are so extensively used in electrochemistry with the necessary assumption that they do not form ion complexes, we considered it important to test the claims of Mohan and Rechnitz. Therefore, we report measurements on the Mg^{++}-ATP stability constant for a test of the pH titration method, and measurements of the Na^{+}-ATP stability constants with varying concentrations of tetrapropylammonium ions to test for binding of the latter to ATP.

CHAPTER II

EXPERIMENTAL

Materials

The tetra-sodium salt of PRPP and the disodium salt of ATP were purchased from the Sigma Chemical Company. Tetrapropylamminium bromide (tpaBr) was purchased from the Eastman Organic Chemical Company, and purified by recrystallizing three times from 98% ethanol. Solutions of tpaBr were prepared and filtered near 70°C, and the crystals collected at room temperature. All other chemicals were of reagent grade. Heavy metal contaminants were extracted from commercial magnesium chloride with dithizone (11) and the magnesium concentration subsequently determined by complexometric titrations with EDTA (ethylenediamine-tetraacetic acid) with Eriochrome Black T as indicator (12). The NaOH which was used as the base titrant in the potentiometric titrations was carbonate free and had been standardized by titration with standard HCl (J. T. Baker DILUTE-IT) using bromothymol blue as end-point indicator. Standard pH solutions were obtained from Fisher (pH 7.0 ± 0.02, pH 10.0 ± 0.02, pH 4.0 ± 0.02) Scientific Company.

Determination of PRPP Impurities

Following the recommendations of Cohn (13), an ion exchange

chromatographic separation of PRPP and its impurities was developed. Solutions of P_i, ribose-5-P_i, PP_i, fructose-1,6-diphosphate, and PRPP, either separately or as mixtures, were used to establish elution conditions. The fructose-1,6-diphosphate served as an analog of ribose-1,5-diphosphate, which was not commercially available. Continuous gradients of ammonium formate at pH 5.0 revealed the conditions used in subsequent batch elutions. The complete batchwise elution of the appropriate compound was verified by collecting a second 100 ml fraction with the same eluant and testing for phosphate. These experiments led to the following procedure.

About 20 μmoles of PRPP (pH 6.0) was applied to a 12 ml bed volume of Dowex-1-2X, formate, 100-200 Mesh anion exchange resin in a 1 cm x 15 cm Pharmacia column. Five fractions were collected by eluting the column with ammonium formate solutions at pH 5 as follows: 1) 100 ml of 0.01 M, 2) 100 ml of 0.1 M, 3) 200 ml of 0.25 M, 4) 100 ml of 0.5 M, and 5) 100 ml of 1.0 M. These fractions should contain: 1) solutes not bound to resin, 2) P_i and ribose-5-P, 3) PP_i and ribose-1,5-diphosphate, 4) PRPP, and 5) any PRPP not eluted in fraction 4. These fractions were then flash evaporated at 45°C until the volume was reduced to 5-7 ml or until ammonium formate crystallized. Aliquots of each fraction were set aside for subsequent determination of ribose, as described below. Duplicate 1 ml aliquots of fractions 1, 2, 3, and 5 were evaporated by a nitrogen stream and irradation from an IR lamp to less than 0.25 ml for phosphate analysis. Triplicate

aliquots (50, 50, and 100 µl) of fraction 4 were used without evaporation. To these aliquots of each fraction, 0.25 ml of 10 N sulphuric acid was added and the fractions heated for one hour at 150°C in a paraffin bath to hydrolyse organic phosphates. If ammonium formate crystallized, more sulphuric acid was added, and if a brown color remained, one drop of 2 N nitric acid was added, and the solution heated for 5 more minutes in 150°C in the paraffin bath. One ml of glass distilled water was then added to each aliquot and the solution heated in a boiling water bath for 10 minutes. The total aliquots were then used for phosphate analysis by the standard Fiske-Subbarow procedure (Sigma, Tentative Technical Bulletin, No. 670, December, 1965).

Ribose quantities in all fractions were measured by the orcinol method to permit calculation of the molar quantities of both the organic and inorganic phosphates in the fractions. The orcinol reagent was prepared as follows. Solution 1: 13.5 g ferric ammonium sulphate and 20 g orcinol (recrystallized from benzene) in 500 ml aqueous solution. Solution 2: 2.5 ml of solution 1, 415 ml concentrated (11.6 M) HCl, diluted to 500 ml with distilled water. Ribose determinations were made by addition of 3.00 ml of solution 2 to 1.00 ml of aliquots containing 50 to 200 nmoles of unknown or ribose-5-P standard. These solutions were heated in a boiling water bath for 20 min, cooled to room temperature and their absorbances measured at 660 nm. Ribose standards consistently gave a slightly lower standard curve than the ribose-5-P standards, therefore, the latter curves were used. Orcinol solution 1 was prepared fresh each week and stored at 5°C; solution 2 was prepared fresh each

time ribose determinations were made.

Results of the phosphate and ribose analysis revealed that the PRPP used in the third determination of stability constants (Set C in Table I) contained the following amounts of impurities calculated as mole % of total moles of PRPP: P_i, 2.0%; ribose-5-P, 2.2%; PP_i, 7.6%; ribose-1,5-diphosphate, 12%.

Determination of ATP Impurities

About 17 μmoles of ATP (pH 7.0) was applied to a 2 ml bed volume of Dowex-1, 8% cross-linked (200-400 mesh) anion exchanger (in chloride form). Five fractions were collected by eluting the column with 50 ml of H_2O, 100 ml of 10 mM NH_4Cl, 100 ml of 0.003 N HCl, 100 ml of 20 mM NaCl in 0.01 N HCl, and 100 ml of 0.2 M NaCl in 0.01 N HCl. Fraction 2 contained adenosine and adenine, fraction 3 contained AMP and inorganic phosphate, fraction 4 contained ADP, and fraction 5 contained ATP. Quantities of each nucleotide were determined by absorbance at 260 nm. Phosphate in fraction 3 was determined by the Fiske-Subbarow procedure as described above. Results of the analysis showed the following percentage of contaminants: no adenine or adenosine; 1% ADP; 0.4% AMP, and 1.3% P_i, each calculated as mole % of the moles of ATP present.

Determination of Metal-Ligand Stability Constants by the pH Titration Method

Titrations of both PRPP and ATP were made with Radiometer (Copenhagen) instruments including: PHM 25/TTT11 titrator, PHA

925a scale expander graduated in 0.01 pH units, TTA31 titration assembly and Radiometer GK2320C combined pH and reference electrode. All titrations were performed in a titration vessel with a water jacket kept at 25°C. Argon, saturated with water by passage through a gas scrubber bottle, was layered on top of the titration solutions which were magnetically stirred.

For PRPP titrations, NaCl was added to a 3.0 mM PRPP solution to give 180 mM in nominal ionic strength, μ, calculated as

$$\mu = 3[MgCl_2]_t + [NaCl]_t$$

where brackets and subscripts indicate total concentrations. About 0.5 ml of 0.1 N HCl was added at the beginning of each titration in order to achieve an initial pH $\simeq$ 4.0; therefore, the total volume for each PRPP titration solution was 10.5 ml. For ATP titrations, tpaBr (tetrapropylammonium bromide) was used instead of NaCl, the total volume was 20.0 ml, and ATP concentration was 1 mM. The titrant normality for PRPP titrations was 0.09874 N NaOH, and 0.04937 N NaOH for ATP titrations, and a maximum of 1 ml titrant was added from a 2.5 ml syringe in each titration. The SUB1 micrometer and syringe (Hamilton No. 1002) were calibrated to within 0.2% precision by weights of water delivered to weighing bottles. Values of pH and micrometer readings were recorded following each increment of titrant.

Data Analysis

Data analysis was done using the least squares computer program

SCOGSII developed in collaboration with Dr. John P. Chandler at our university. SCOGSII is a modified version of SCOGS (14). SCOGSII differs from Sayce's SCOGS in that: 1) it uses a better minimizer (MARQ), and 2) it allows any other constants ("parameters") to be least-square fitted, whereas Sayce's SCOGS allows only the stability constants to be fitted.

Data analyzed by both programs were shown to produce identical results when constants other than stability constants were the same. SCOGSII is capable of calculating simultaneously, or individually, association constants for any of the species formed in systems containing up to four metals and four ligands, provided that the degree of complex formation is pH-dependent. Thus it may be used to analyze appropriate pH titration data to yield acid association constants (and hence pka's). Metal-ion hydrolysis constants, and stability constants of metal-ligand complexes. The output includes the chi-square value of the fit (see Appendix A), the best fit values of each fitted parameter with estimated standard deviations, the correlation coefficients between each pair of parameters, and a complete table giving at each experimental pH the calculated concentrations of all species (for free ligands and metals and all complexes). Generally, σ(pH), which is the standard deviation for pH, is approximately $\pm$ 0.03 for all of our pH titrations. A schematic and explanation of SCOGSII is given in Appendix A.

CHAPTER III

RESULTS AND DISCUSSION

Mg^{2+} and H^{+} Stability Constants of PRPP Complexes

The following model was used for analyzing titration data on PRPP.

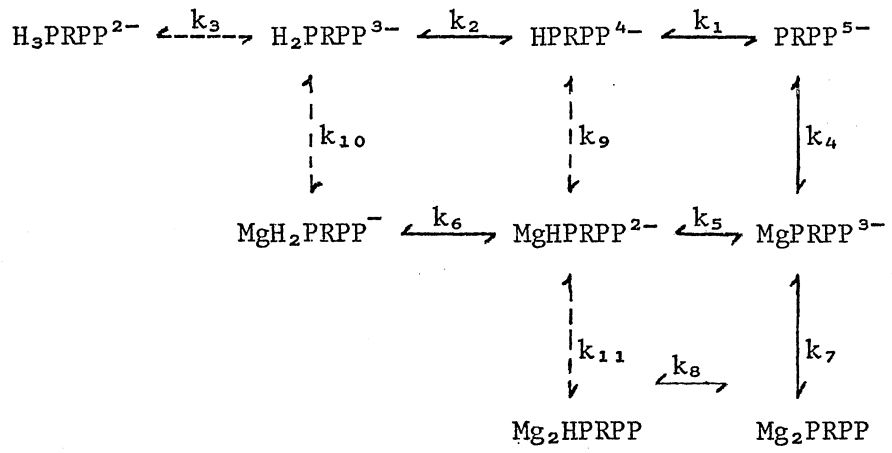

where k are the stepwise association (stability) constants. The constants of equilibria shown by dashed arrows are determined by the other constants since they form a closed cycle over which the free energy change is zero. Stated another way, the free energy change in going from any species to another is independent of the path. Thus, e.g.,

$$\log k_1k_9 = \log k_4k_5$$

The overall stability constant, $\beta(J)$, of a species J equals the product of the stepwise stability constants in going from the free ligand to the J^{th} species. For example,

$$\beta_6 = k_4k_5k_6 = \frac{(MgH_2PRPP)}{[H^+]^2(Mg^{2+})(PRPP)}$$

where parentheses denote molar concentrations and $[H^+]$, the hydrogen ion activity, is taken as antilog (-pH).

The concentrations of H_3PRPP^{2-} and Mg_2HPRPP never rose above 0.5% of the total PRPP at any titration point with reasonable stability constants and, therefore, these stability constants were fixed at reasonable values. Omitting these species from the model is, therefore, justified.

Results of fits to all three PRPP experiments are shown in Table I. Raw data for set C are summarized in Table II. The effects of the PP_i and ribose-1,5-diphosphate impurities in the latest data set (set C in Table I) were included in the model as ligands 2 and 3 (L2 and L3), respectively. The log of overall stability constants (log β) for PP_i were taken from Thompson's data (6) as follows: L2•H, 8.51; L2•H_2, 14.79; L2•Mg, 5.08; L2•Mg•H, 11.6; L2•Mg_2, 7.41. The log β values for ribose-1,5-diphosphate were estimated from data on fructose-1,6-diphosphate (17) as follows: L3•H, 6.56; L3•H_2, 12.39; L3•Mg, 2.73; L3•H•Mg, 9.29; L3•Mg_2, 4.87. To test the sensitivity of the model to uncertainties in these constants for the impurities, each stepwise constant for ribose-1,5-diphosphate was doubled and the data refitted. The resulting best fit constants were not significantly different from the results in

TABLE I

PRPP H^+ AND Mg^{2+} APPARENT STEPWISE STABILITY CONSTANTS AT 25°C

Set[a]	Analysis	log k_1	log k_2	log k_4	log k_5	log k_6	log k_7
A	SCOGS	6.74	5.87	3.25	6.23	3.78	1.64
B	SCOGS	6.48 ± 0.01	5.73 ± 0.01	3.17 ± 0.04	6.34 ± 0.06	4.20 ± 0.11	1.73 ± 0.08
C	SCOGSII	6.52 ± 0.02	5.91 ± 0.02	3.16 ± 0.03	6.25 ± 0.04	4.15 ± 0.12	1.60 ± 0.06

[a]Set A data are by Thompson, with results corrected for Li^+ binding as explained under Experimental. Set B data are by Blanton, and set C data are by Li.

TABLE II

PRPP TITRATION DATA AT CONSTANT IONIC STRENGTH (~ 180 mM)

Titration I[a]		Titration II[b]		Titration III[c]		Titration IV[d]	
Micrometer Reading	pH	Micrometer Reading	pH	Micrometer Reading	pH	Micrometer Reading	pH
0.543	5.145	0.758	4.721	1.046	4.379	2.668	3.860
1.497	5.379	2.196	5.085	4.703	5.139	9.079	5.000
4.412	5.848	3.573	5.439	7.700	5.601	12.773	5.620
7.185	6.189	6.241	5.751	9.332	5.849	15.073	6.070
8.730	6.369	8.416	6.046	11.016	6.117	15.712	6.248
11.359	6.715	10.286	6.303	12.805	6.431	16.567	6.539
12.979	7.010	12.772	6.715	14.119	6.737	17.200	6.905
13.907	7.260	14.199	7.080	14.750	6.941	17.445	7.149
14.580	7.535	14.927	7.398	15.212	7.158		
15.000	7.818	15.348	7.720	15.734	7.528		
15.288	8.153	15.692	8.162	15.980	7.878		

TABLE II (continued)

---

[a] 2.86 mM Na_5PRPP, 171.41 mM NaCl, no $MgCl_2$, Temperature at 25°C.

[b] 2.86 mM Na_5PRPP, 162.41 mM NaCl, 2.86 mM $MgCl_2$, Temperature at 25°C.

[c] 2.86 mM Na_5PRPP, 142.85 mM NaCl, 9.52 mM $MgCl_2$, Temperature at 25°C.

[d] 2.86 mM Na_5PRPP, 57.14 mM NaCl, 171.42 mM $MgCl_2$, Temperature at 25°C.

Table I. The effects of 1% systematic errors in the titrant normality, total PRPP concentration, and micrometer calibration were also tested by changing these constants and refitting. These errors did not cause significant changes in the stability constants even though the quality of fits were poorer as judged by the chi-square values.

The step stability constants for MgPRPP and Mg_2PRPP are sufficiently close to literature values for Mg^{2+} complexes of ADP and glucose-1-P (Table III) to suggest that the two Mg^{2+} binding sites on PRPP are the 1-PP and 5-P groups which are acting rather independently.

The effects of competing protons and alkali metal ions (M) on the Mg^{2+}-ligand stability constants are given by the relation (18),

$$\text{app-}k_{MgL} = \frac{k_{MgL}}{1 + k_{HL}[H^+] + k_{ML}(M)}$$

where appk and k are the apparent and true association constants, respectively, and

$$\text{app-}k_{MgL} \equiv \frac{(MgL)}{(Mg^{2+})[(L) + (HL) + (ML)]}$$

Thus the concentrations of MgL may be calculated for any pH and alkali metal ion concentration if k_{HL} and k_{ML} are known.

In Table III, the Mg^{2+} stability constants of ADP and glucose-1-P were corrected for competitive binding of Na^+ by using the k_{NaL} values of Smith and Alberty (19) for ADP and AMP, which give corrections of -0.33 and -0.17 in log k values with 0.17 M Na^+ ions. The

TABLE III

COMPARISON OF Mg^{2+}-LIGAND STEPWISE STABILITY CONSTANTS.
APPARENT CONSTANTS WITH 0.170 M NaCl AND 0.20 M IONIC STRENGTH

	MgPRPP	MgADP[a]	Mg_2PRPP	MgGlucose-1-P[b]
log k	3.16	3.17	1.6	1.9

[a] Ref. 15 corrected by -0.33 log k units for Na^+ binding.

[b] Ref. 16 corrected by -0.17 log k units for Na^+ binding.

Na^+ and K^+ ligand stability constants for organo-phosphates are close enough to use them interchangeably. Although the stability constants of Smith and Alberty (20) for nucleotide-divalent metal ion complexes appear to be in serious error (see Table VI in Ref. 15), their results with alkali metal ion-nucleotide complexes (19) appear to be accurate, judging from the fact that we obtain the same $NaATP^{3-}$ stability constant as discussed below.

Experiments Testing Validity of the pH Titration Method

In order to demonstrate whether the pH titration method is accurate for determining metal-ligand stability constants, we designed experiments to directly compare results from the pH titration method with those from the Mg^{2+} selective electrode method. However, it was shown (21) that pH measurements are unreliable at low ionic strength (μ), whereas the Mg^{2+} selective electrode does not respond to Mg^{2+} at high μ (E. Li, unpublished results). Thus a direct comparison was not practical. Data on Mg^{2+}-ATP solutions at 0.18 M ionic strength by the pH titration method were obtained, however, to compare results with other determinations of the MgATP stability constant. The model is shown in Figure 1 together with the best fit constants obtained. Raw data are shown in Table IV. When a Mg_2ATP complex was added to the model it forced the sum of squares to larger values unless its step stability constant was kept negligible.

A comparison of the MgATP stability constant of this study

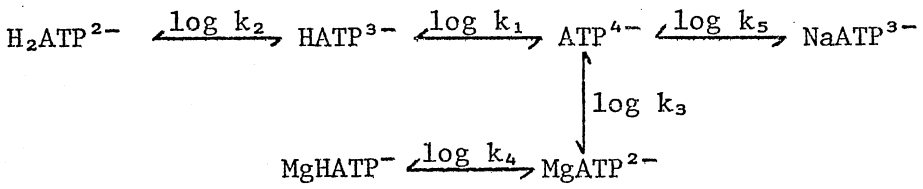

$\log k_1 = 7.05 \pm 0.02$

$\log k_2 = 3.95 \pm 0.04$

$\log k_3 = 5.06 \pm 0.03$

$\log k_4 = 4.76 \pm 0.05$

$\log k_5 = [1.21]^a$

[a]Fixed value.

Figure 1. ATP H^+ and Mg^{2+} Stepwise Stability Constants. Results obtained from analysis of ATP titrations performed at 25°C; 0, 1.18, and 20 mM of $MgCl_2$ corresponding to 180, 177, 120 mM of tetrapropylammonium bromide, respectively. All titrations were with 1 mM Na_2H_2ATP.

TABLE IV

Mg-ATP TITRATION DATA AT CONSTANT IONIC STRENGTH (~ 180 mM)

Titration I		Titration II		Titration III	
Micrometer Reading	pH	Micrometer Reading	pH	Micrometer Reading	pH
9.113	4.441	11.521	4.560	14.996	4.597
10.506	4.775	13.622	4.861	17.964	4.939
11.331	5.118	15.185	5.100	19.631	5.200
12.348	5.739	17.197	5.405	20.808	5.440
12.654	5.882	19.129	5.738	21.572	5.661
13.132	6.086	20.524	6.055	21.965	5.961
13.785	6.289	21.584	6.400	22.492	6.570
15.591	6.675	22.187	6.714	22.828	7.921
17.573	7.005	22.588	7.085	22.882	8.251
19.137	7.260	22.800	7.460		
20.962	7.621	23.083	8.657		
21.672	7.823				
22.292	8.085				

with results from other reports is given in Table V. These selected results and others from the summary in reference (15) indicate that the criticisms of the pH titration method by Mohan and Rechnitz (9) are unwarranted. The unusually low values of Smith and Alberty (20) for all the divalent metal-nucleotide complexes are most likely the result of inaccuracies in the mathematical analysis method, which were limited to approximation methods at that time. Currently more exact mathematical analysis is possible with computer methods. Our results are in excellent agreement with those of O'Sullivan and Perrin (22). Mohan and Rechnitz feel that the pH titration method is less sensitive than the divalent metal ion electrode method, which has indicated higher stability constants. Yet the pH titration method has given the highest estimates of the MgATP stability constant at physiological ionic strengths of any method. A direct comparison of the pH titration and divalent metal electrode methods is not possible, since present data are limited to high ionic strength for the pH titration method, and low ionic strength for the divalent metal ion electrode. The extensive data of Phillips *et al.* (15) are considered to provide the most reliable constants for extrapolating to zero ionic strength. Such an extrapolation of our MgATP stability constant gives a log k value of 6.27 at zero ionic strength which is actually higher than, but in good agreement with the value of 6.06 obtained by Mohan and Rechnitz.

It should be noted that the effect of Na^+ from the Na_2H_2ATP used in our experiments was a lowering of the log k of MgATP by only 0.03 units due to competitive binding of Na^+ to ATP if the NaATP stability constant (16.2 M^{-1}) determined as indicated below is used.

TABLE V

SELECTED STABILITY CONSTANTS REPORTED FOR THE Mg^{2+} COMPLEX FORMATION REACTION OF ATP

Method	Condition	Temp.	log K	Ref.
pH titration	0.2M tpaBr	25°C	3.47±0.03	(20)
pH titration	0.1M tpaBr	30°C	5.02±0.06	(23)
pH titration	0.2M tpaBr	25°C	5.06±0.03	This Thesis
Resin competition	0.1M tpaBr	25°C	4.60±0.03	(15)

Thus uncertainty in the true NaATP constants introduces negligible error in the results.

Evidence For or Against a Mg_2ATP Species

Mohan and Rechnitz (10) consider they have good evidence for a Mg_2ATP species with a step stability constant of 400 ± 40 at zero ionic strength. They suggest that the pH titration method is insensitive to such species not involving a displacement of protons. We argue, however, that the method is not necessarily insensitive to such species since they exist in coupled equilibria with species containing protons. The results with our analysis when a Mg_2ATP species was added to the model support this view. If the method were insensitive to this species the sum of squares (PHI) would not have been affected by its presence. Instead PHI was approximately doubled by assuming a step stability constant as little as 3. Since some of the titration data contained 60 mM Mg^{2+}, we conclude, in agreement with most other binding studies of MgATP systems, that Mg_2ATP does not exist at significant concentrations. Error analysis of the divalent metal ion electrode method (unpublished results) indicates that significant, and probably large systematic errors are virtually impossible to avoid in this method. Thus we doubt that the evidence for a Mg_2ATP species is good.

Evaluation of the Possible Association of Tetrapropylammonium Ions with ATP

Mohan and Rechnitz (9) suggest that association of the tetraalkylammonium ions with phosphate ligands is one of the two possible

causes for the large discrepancies in metal-ligand binding constants they find in comparison to previous reports. This is an important question to clarify since it is often necessary to use a salt to increase the ionic strength of a solution without forming any new complexes. The accuracy of an enormous amount of published data depend on the validity of the assumption that association of these quaternary ammonium ions (Q^+) with anionic ligands is negligible. Alberty and Smith (19) thought their data on the stability constants of alkali metal ion-ligand complexes demonstrated that Q^+-L formation was negligible. They studied stability constants of Me^+-L complexes, using various concentrations of Q, but at constant ionic strength, where $Me^+ = Na^+$, K^+, and Li^+, and L = HPO_4, AMP, ADP, ATP, and AQP (adenosine tetraphosphate). Thus they measured stability constants for each complex in four separate solutions, where concentrations, $(Q^+) + (Me^+) = 0.200$ M always, but the % of this 0.200 M contributed by Q^+ was varied as: 1) 0% Q^+, 2) 25% Q^+; 3) 50% Q^+, and 4) 75% Q^+. The stability constants were the same in all four solutions, which led them to conclude that Q^+-L complex formation was negligible in spite of the high charge density of these phosphates.

Contrary to this reasonable intuition, however, we claim that the results Smith and Alberty obtained would occur no matter what the stability constants of Q^+-L were. Varying (Q^+) <u>with the constraint</u> $(Q^+) + (Me^+) = \mu$, a <u>constant</u> ionic strength, will not, therefore, provide any evidence for or against Q^+-L complexes. Proof of this claim is given in Appendix B. Thus to estimate K_Q from pH titration data, it is necessary to vary μ. As explained in Appendix B, variations in μ normally introduce another uncertainty, the variations

in activity coefficients of ionic species. However, between approximately 0.1 and 0.2 M ionic strength, activity coefficients are generally fairly constant. The thermodynamic data of Phillips et al. (Table IV in Ref. 15) indicate that there is no significant change (± 0.04) in the log stability constant of $HATP^{3-}$ between an ionic strength of 0.090 and 0.180 M. The Na^{+}-ATP^{4-} and Q^{+}-ATP^{4-} association equilibria are of the same charge type as H^{+}-ATP^{4-}, so we would also expect little change in the activity coefficients of these ionic species, or in the stability constants of $NaATP^{3-}$ and $QATP^{3-}$ complexes between μ = 0.090 and 0.180 M. Accepting this assumption, we are free to vary (Q^{+}) and (Na^{+}) independently within this range of μ, which permits us to determine k_Q, k_{Na^+}, and k_{H^+}, as explained in Appendix B. The experimental protocal is given in Table VI.

The model including the Q-ATP^{3-} complex, is

$$H_2ATP^{2-} \overset{k_2}{\rightleftharpoons} HATP^{3-} \overset{k_1}{\rightleftharpoons} ATP^{4-} \overset{k_3}{\rightleftharpoons} NaATP^{3-}$$

$$ATP^{4-} \overset{k_4}{\updownarrow} QATP^{3-}$$

Analysis of the data in Table VII gave a stability constant for $k_{QATP} = k_4$ essentially zero, and $k_3 = 17\ M^{-1}$. To see how sensitive the data were to assumed values of k_{QATP}, fits were also obtained with k_{QATP} fixed at 1.0, 2.0, 4.0 and 7.9 M^{-1}. Chi-square values of these fits were increased by 10% with k = 2.0 M^{-1}, and doubled at k = 4.0 M^{-1}. Therefore, we suspect that tetrapropylammonium ions do not significantly complex with ATP^{4-}. Competitive binding of Q^{+} to a ligand (e.g., ATP) would reduce metal- (or proton-) ligand

TABLE VI

EXPERIMENTAL PROTOCAL FOR Na^+-tpa^+-ATP pH TITRATIONS AT 25°C

	Titrations				
	I	II	III	IV	V
Na_2H_2ATP	3.5 mM	3.5 mM	3.5 mM	3.5 mM	3.5 mM
NaBr	90 mM	180 mM	0 mM	0 mM	90 mM
tpaBr	0 mM	0 mM	90 mM	180 mM	90 mM
Total Volume	7.50 ml	7.50 ml	7.50 ml	7.50 ml	7.50 ml

TABLE VII

Na^+-tpa^+-ATP TITRATION DATA

Titration I		Titration II		Titration III		Titration IV		Titration V	
Micrometer Reading	pH	Micrometer Reading	pH	Micrometer Reading	pH	Micrometer Reading	pH	Micrometer Reading	pH
3.029	4.102	18.690	4.854	4.673	4.570	18.000	5.216	4.208	4.420
4.061	4.357	19.180	5.090	5.265	4.831	18.646	5.877	5.271	4.809
5.164	4.669	19.668	5.353	5.662	5.093	19.197	6.232	6.270	5.444
6.367	5.226	20.652	5.801	5.968	5.391	20.389	6.666	6.689	5.709
7.062	5.655	21.161	5.973	6.263	5.716	22.104	7.154	7.577	6.102
8.582	6.260	22.137	6.260	6.704	6.085	23.709	7.760	10.758	6.995
9.740	6.570	23.067	6.501	7.023	6.277	24.308	8.268	11.618	7.333
10.910	6.885	23.765	6.685	9.185	7.001			12.151	7.675
12.230	7.372	24.855	7.055	10.150	7.300			12.415	7.968
12.904	7.936	25.244	7.026	10.988	7.610			12.496	8.112
		25.710	7.640	11.543	7.921				
		25.816	7.780	11.848	8.200				

stability constants, k_{ML}, by the following (see Appendix B),

$$\text{app } k_{ML} = \frac{k_{ML}}{1 + k_{QL}(Q)}$$

If measurements were made with (Q) at 0.18 M to give nearly physiological ionic strengths, and k_{QL} were even as high as 4.0 M^{-1}, k_{ML} would be reduced by 42% (app k_{ML} = 0.58 k_{ML}) only, and k_{QL} is probably considerably lower.

The best fit value of k_{NaATP} was 17 ± 0.5 M^{-1} in good agreement with the 14.3 M^{-1} value of Smith and Alberty (19) at essentially the same ionic strength (0.2 M). Mohan and Rechnitz (9) obtained a value of 230 ± 20 M^{-1} for k_{NaATP} at infinite dilution using the Na^+ glass electrode. They claim (9) that this difference cannot be ascribed to activity coefficient differences which they estimate would change k by only 2-fold from μ = 0.01 to 0.2 M. This is a gross miscalculation, however, as even their equations (1) and (8) predict a 5.8-fold change in k. We could use the extensive studies of Phillips et al. (15) again to estimate the change in k_{NaATP} from μ = 0 to 0.2 M, by assuming that the species in $H^+ + ATP^{4-} \longleftrightarrow HATP^{3-}$, and $Na^+ + ATP^{4-} \longleftrightarrow NaATP^{3-}$ equilibria have the same change in activity coefficients, since they have the same charge types. The k_{HATP} changes by a factor of 4.3 for this change in μ. Thus, our result at $\mu \simeq 0.2$ M for k_{NaATP} would predict a value of 73 M^{-1} at μ = 0, which is 3 fold less than the value of Mohan and Rechnitz. Since our results with the pH titration method for MgATP are so close to accepted values, and our data on Na^+-, Q^+-ATP argue against

$QATP^{3-}$ complex formation, we doubt that the remaining difference is due to the factors they suggested (10). The activity coefficients of species in solution with high charged ions (4- for ATP) depend specifically on the chemical identity of the ions, in contrast to solutions of lower charge type (2 or less). Thus, it is quite possible that the extrapolation based on the H^+-ATP^{4-} system is sufficiently different for the Na^+-ATP^{4-} system to explain the difference between the predicted NaATP stability constant at $\mu = 0$ and that measured by Mohan and Rechnitz at very low μ and extrapolated to $\mu = 0$. Otherwise, the difference is due to experimental error in either or both measurements. The discrepancy is not nearly as large as they suggested, however.

A SELECTED BIBLIOGRAPHY

(1) Veloso, D., Guynn, R. W., Oskarsson, M., and Veech, R. L. (1973) J. Biol. Chem. 248, 4811-4819.

(2) Krewitsky, T. A., Neil, S. M., Elion, G. B., and Hitchings, G. H. (1969) J. Biol. Chem. 244, 4779-4784.

(3) Holmes, E. W., McDonald, J. A., McCord, J. M., Wyngaarden, J. B., and Kelly, W. N. (1973) J. Biol. Chem. 248, 144-150.

(4) Berlin, R. D. (1969) Arch. Biochem. Biophys. 134, 120-129.

(5) Switzer, R. L. (1971) J. Biol. Chem. 246, 2447-2458.

(6) Thompson, R. E. (1974) Ph.D. Thesis, Oklahoma State University, Stillwater, Oklahoma.

(7) Cookson, R. F. (1974) Chem. Rev. 74, 5-28.

(8) Khorana, H. G., Fernades, J. F., and Kornberg, A. (1958) J. Biol. Chem. 230, 941-948.

(9) Mohan, M. S., and Rechnitz, G. A. (1970) J. Amer. Chem. Soc. 92, 5839-5842.

(10) Mohan, M. S., and Rechnitz, G. A. (1970) Arch. Biochem. Biophys. 162, 194-199.

(11) Morrison, J. F. and Uhr, M. L. (1966) Biochim. Biophys. Acta 122, 57-74.

(12) Skoog, D. A., and West, D. M. (1969) Fundamentals of Analytical Chemistry, 2nd Ed., p. 343. Holt, Rinehart and Winston, Inc., New York.

(13) Cohn, W. E. (1957) in Methods in Enzymology, Colowick, S. P., and Kaplan, N. O., ed., Vol. 3, p. 724-747. Academic Press, New York.

(14) Sayce, I. G. (1968) Talanta 15, 1397-1411.

(15) Phillips, R. C., George, P., and Rutman, R. J. (1966) J. Amer. Chem. Soc. 88, 2631-2640.

(16) Clark, H. B., Cusworth, D. C., and Datta, S. P. (1954) Biochem. J. 58, 146-154.

(17) McGilvery, R. W. (1965) Biochemistry 4, 1924-1930.

(18) Johnson, M. J. (1960) The Enzymes 3, 408-417.

(19) Smith, R. M., and Alberty, R. A. (1956) J. Phys. Chem. 60, 180-183.

(20) Smith, R. M., and Alberty, R. A. (1956) J. Phys. Chem. 78, 2276-2380.

(21) Hill, D. E., and Spivey, H. O. (1974) Anal. Biochem. 57, 500-505.

(22) O'Sullivan, W. J., and Perrin, D. D. (1964) Biochemistry 3, 18-26.

(23) O'Sullivan, W. J., and Perrin, D. D. (1961) Biochim. Biophys. Acta 52, 612.

(24) Marquardt, D. W. (1963) J. S. I. A. M. 11, 431.

(25) Davis, C. W. (1962) Ion Association, pp. 38-48. Butterworth, London.

APPENDIXES

APPENDIX A

A SCHEMATIC AND EXPLANATION OF SCOGSII

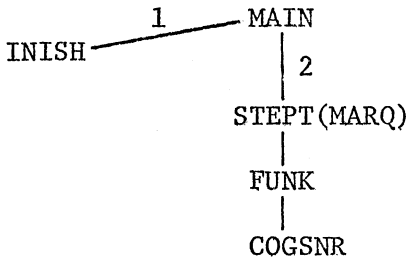

MAIN - The main program takes care of input and output quantities

INISH - A subroutine to specify all the initial estimates for the parameters to be fitted. INISH returns to MAIN which then calls STEPT(MARQ)

STEPT(MARQ) - The minimizer subprogram (see below for details)

FUNK - Subroutine FUNK calculates PHI, the function to be minimized

COGSNR - A subroutine subprogram called by FUNK to solve the simultaneous equations (1) and (3) below to obtain free ligand and metal ion concentrations

The analysis begins in COGSNR with calculation of the right hand side (RHS) of the Ligand Conservation Equation (1) for each ligand present at each pH point in the course of the titration.

$$L_t(I) = L_f(I) + \sum_{J=1}^{N} ML(I,J)C(J) \qquad (1)$$

$$\text{with } C(J) = \beta(J)L_f(I)^{ML(I,J)}M_f(I)^{MM(I,J)}\ (H^+)^{-MN(J)} \qquad (2)$$

where $L_t(I)$ = total concentration of ligand of type (I)

$L_f(I)$ = concentration of free ligand of type (I)

N = number of complex species

ML(I,J) = number of ligands of type (I) in the complex species J

MM(I,J) = number of metals of type (I) in the complex species J

MN(J) = - the number of protons or + the number of hydroxyls in the J^{th} complex species

$C(J)$ = concentration of the J^{th} complex species

$M_f(I)$ = concentration of free metal (I)

$\beta(J)$ = overall association constant for the J^{th} complex species

A metal conservation equation is also required for each metal present in the system.

$$M_t(I) = M_f(I) + \sum_{J=1}^{N} MM(I,J)C(J) \qquad (3)$$

where $M_t(I)$ = total concentration metal of type (I)

Subroutine COGSNR solves the above simultaneous equations by a Newton-Raphson procedure using the current estimates for the stability constants. The concentrations of all free ligands and metals are adjusted until convergence, whereupon the RHS's of equations (1) and (3) are all equal to their lefthand side (LHS), the known total concentration for each type of ligand or metal. These concentrations of $L_f(I)$ and $M_f(I)$ permit the calculation of concentrations of all

complex species C(J) by equation (2). The C(J)s are then used to calculate the residuals from the "analytical hydrogen ion concentration equation",

$$\text{ACID-BASE} + \sum_{I=1}^{NL} L_t(I)NDP(I) = (H^+)-(OH^-)- \sum_{J=1}^{N} MN(J)C(J) \qquad (4)$$

where ACID = amount of acid added during the course of titration

BASE = amount of base added during the course of titration

NL = total number of ligands

NDP(I) = number of displaceable protons in the ligand complex initially added (e.g., NDP(I) = 2 for Na_2H_2ATP)

$OH^- = \frac{K_w}{H^+}$, where K_w is the hydrolysis product of water.

The residual, R(I), is then calculated at each titration point I as

$$R(I) = HO_c(I) - HO_e(I)$$

where HO_c and HO_e are the left and right hand sides of equation (4) representing the calculated and experimental hydrogen ion concentrations, respectively.

In practice, however, we use

R(I) = (actual titre of base) - (titre calculated from HO_e) since the variance of R(I) is not expected to change as markedly during a series of experiments as it does when R(I) is defined in terms of analytical hydrogen ion concentration (14).

Equation (4) is a general expression of the electroneutrality con-

dition, which is valid for all charge types. Hence it is a problem independent statement of the electroneutrality equation.

The sum of squares, PHI, is then calculated. PHI is defined as

$$\sum_{I=1}^{NPTS} [R(I)/YSIG(I)]^2 \qquad (5)$$

where YSIG(I) is the estimate of experimental error in $HO_{exp}(I)$. The minimizer MARQ calculates the next estimates of the adjustable parameters (i.e., stability constants and other constants as desired, e.g., titrant normality, etc.) using the algorithm of Marquardt (24). Gradient methods such as those used by MARQ obtain this estimate by calculating the rates of change in PHI with respect to the adjustable parameters, α_i; i.e.,

$$\frac{\partial PHI}{\partial \alpha_i} \text{ for } i = 1, \ldots, NPAR \qquad (6)$$

where NPAR = number of adjustable parameters. From these derivatives, the increment in each parameter is calculated, and the updated parameter values used in the next iteration of the above calculations, starting with the solutions of equations (1) and (3) again. These iterations are repeated until PHI converges to a minimum. The parameter values; α_i, at the minimum in PHI are the least squares "best fit" values, and at this minimum, PHI = chi square (χ). A chi-square equal to the number of degrees of freedom (data points minus adjustable parameters) corresponds to a 50% probability of obtaining a worse fit (chi square probability = 0.5). A chi-square probability

greater than approximately 0.1 is considered an acceptable fit by this criterion.

APPENDIX B

PROOF THAT THE IONIC STRENGTH MUST BE VARIED TO DETERMINE THE STABILITY CONSTANT OF Q-L

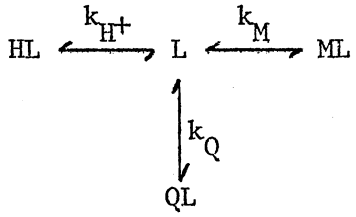

The apparent stability constant is defined as

$$\text{app-}k_{H^+} \equiv \frac{(HL)}{[H^+][(L) + (ML) + (QL)]} \qquad (1)$$

where ( ) denotes concentrations and [ ] denotes activity of H^+ (10^{-pH}). Concentrations of each and of all complexes can be expressed in terms of "stepwise" stability constants, K, and concentrations of free ligand L. Thus expressing app-k_{H^+} (Equation 1) as function of metal ions (M) and (Q) and constants k_M and k_Q,

$$(ML) = k_M(M)(L)$$

$$(QL) = k_Q(Q)(L)$$

which upon substitution in equation (1) yields

$$\text{app-}k_{H^+} = \frac{k_{H^+}}{[1 + k_M(M) + k_Q(Q)]} \qquad (2)$$

where k_{H^+} is the true equilibrium constant, $k_{H^+} \equiv \frac{(HL)}{[H^+](L)}$ independent of (M) and (Q).

Using the definition, $\frac{1}{app\text{-}k_{H^+}} \equiv app\text{-}K^d_{H^+}$ (apparent dissociation constant), equation (2) can be rewritten as

$$app\text{-}K^d_{H^+} = [1 + k_Q(Q) + k_M(M)]K^d_{H^+} \tag{3}$$

which represents a measured quantity ($app\text{-}K^d_H$, the dependent variable) as a function of independent variables (M) and (Q). If (M) and (Q) are varied independently, one can calculate all 3 constants: k_{H^+}, k_Q, and k_M. These constants can also be obtained graphically (see Figure 2).

However, if (Q) and (M) are not independent, e.g., if (Q) and (M) = μ, where μ is a <u>constant</u> ionic strength, then equation (2) becomes

$$app\text{-}k_{H^+} = \frac{k_{H^+}}{1 + k_M[\mu\text{-}(Q)] + k_Q(Q)}$$

$$= \frac{k_{H^+}}{1 + k_M\mu + (k_Q - k_M)(Q)}$$

and

$$app\text{-}K^d_H = [1 + k_M\mu + (k_Q\text{-}k_M)(Q)]K^d_H \tag{4a}$$

or

$$= [1 + k_Q\mu + (k_M\text{-}k_Q)(M)]K^d_H \tag{4b}$$

if (Q) rather than (M) is eliminated. Equations 4a and 4b, however,

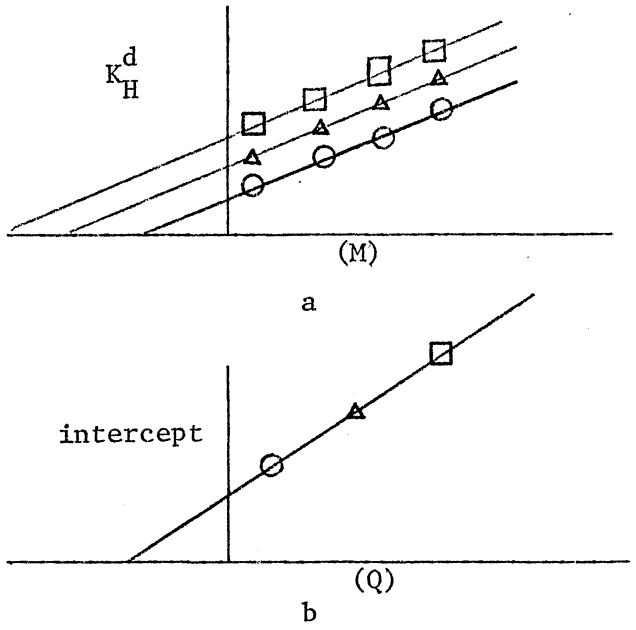

Figure 2. Determination of k_H, k_Q, and k_M by Graphical Interpolation. ▫, Δ, and o are arbitrary data points for illustrations only. A. Primary plot of K_H^d vs (M) at various levels of (Q). Slope = $\frac{k_M}{k_H}$; intercept = $[1 + k_Q(Q)_i]/k_H$

b. Secondary plot of Intercept (obtained from A) vs Q. Slope = $\frac{k_Q}{k_H}$; intercept = $\frac{1}{k_H}$.

are linear functions of only a single independent variable, from which only two of the three constants, k_M, k_Q, and K_H^d may be determined or a linear relation between any two, e.g., $k_{Na^+} = ak_Q + b$, where a and b are constants. Thus the data can be described just as well by any value of k_Q. If μ could be varied, both k_Q and k_M could be calculated, if the variation in activity coefficients with μ were known. Although activity coefficients for univalent and divalent ions may be predicted from theory up to 0.1 M (and some to 0.2 M) ionic strength (25), the variations in activity coefficient with μ for higher charged ions (ADP^{3-}, ATP^{4-}, etc.) are unknown and different for each ion and counterion composition. These activity coefficients could be determined experimentally for each system, but only if Q is known to not bind significantly to L. These considerations explain the central importance of obtaining a reliable method to establish whether an electrolyte used as an ionic strength adjustor binds to the ions under study. Unless such evidence can be provided, the extents of complexation of any M-L system with charged species above 2 will be uncertain. Furthermore there are few ions with as low a surface charge density as the tetrapropylammonium ion, which are soluble enough to provide the 0.2 M ionic strengths desired.

VITA[2]

Edwin Lung-Fat Li

Candidate for the Degree of

Master of Science

Thesis: I. STEADY-STATE KINETIC MECHANISM OF GLYCERALDEHYDE-3-PHOSPHATE DEHYDROGENASE

II. MAGNESIUM AND PROTON STABILITY CONSTANTS OF ORGANIC PHOSPHATE METABOLITES

Major Field: Biochemistry

Biographical:

Personal Data: Born in Hong Kong, December 12, 1951, the son of Yin-Nor and Sui Li.

Educational: Graduated from St. Mary's Grammar School, Southampton, England in 1971; received the Bachelor of Science degree in Biochemistry from Oklahoma State University, Stillwater, Oklahoma in 1975; completed requirements for the Master of Science degree in December, 1977.

Professional Experience: Served as undergraduate research participant at Oklahoma State University, 1974-1975; served as graduate research assistant in Biochemistry, teaching assistant in Chemistry at Oklahoma State University, 1976-1977.